Coupling Capillary Zone Electrophoresis with Electron Transfer Dissociation and Activated Ion Electron Transfer Dissociation for Top-Down Proteomics

ARTICLE *in* ANALYTICAL CHEMISTRY · MAY 2015

Impact Factor: 5.64 · DOI: 10.1021/acs.analchem.5b00883

analytical chemistry

Article

pubs.acs.org/ac

Coupling Capillary Zone Electrophoresis with Electron Transfer Dissociation and Activated Ion Electron Transfer Dissociation for Top-Down Proteomics

Yimeng Zhao,[†,⊥] Nicholas M. Riley,[‡,⊥] Liangliang Sun,[†] Alexander S. Hebert,[‡] Xiaojing Yan,[†] Michael S. Westphall,[‡] Matthew J. P. Rush,[‡] Guijie Zhu,[†] Matthew M. Champion,[†] Felix Mba Medie,[§] Patricia A. DiGiuseppe Champion,[§] Joshua J. Coon,[‡] and Norman J. Dovichi*[,†]

[†]Department of Chemistry and Biochemistry, University of Notre Dame, Notre Dame, Indiana 46556, United States

[‡]Department of Biomolecular Chemistry, Genome Center of Wisconsin, and Department of Chemistry, University of Wisconsin, Madison, Wisconsin 53706, United States

[§]Department of Biological Sciences, University of Notre Dame, Notre Dame, Indiana 46556, United States

Supporting Information

ABSTRACT: Top-down proteomics offers the potential for full protein characterization, but many challenges remain for this approach, including efficient protein separations and effective fragmentation of intact proteins. Capillary zone electrophoresis (CZE) has shown great potential for separation of intact proteins, especially for differentially modified proteoforms of the same gene product. To date, however, CZE has been used only with collision-based fragmentation methods. Here we report the first implementation of electron transfer dissociation (ETD) with online CZE separations for top-down proteomics, analyzing a mixture of four standard proteins and a complex protein mixture from the *Mycobacterium marinum* bacterial secretome. Using a multipurpose dissociation cell on an Orbitrap Elite system, we demonstrate that CZE is fully compatible with ETD as well as higher energy collisional dissociation (HCD), and that the two complementary fragmentation methods can be used in tandem on the electrophoretic time scale for improved protein characterization. Furthermore, we show that activated ion electron transfer dissociation (AI-ETD), a recently introduced method for enhanced ETD fragmentation, provides useful performance with CZE separations to greatly increase protein characterization. When combined with HCD, AI-ETD improved the protein sequence coverage by more than 200% for proteins from both standard and complex mixtures, highlighting the benefits electron-driven dissociation methods can add to CZE separations.

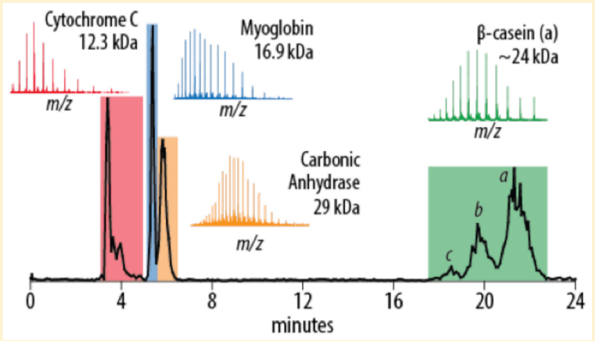

Capillary zone electrophoresis (CZE)[1−4] has emerged as a potential alternative to traditional reversed- phase liquid chromatography (RPLC), especially for front-end separations of proteins in top-down proteomic experiments. Separation based on mass-to-charge (m/z) rather than hydrophobic interactions lends high resolving power to CZE to separate for the diversity of proteoforms seen in a protein mixture, because proteins with minor sequence variations or post-translational modifications (PTMs) often have similar hydrophobicities but different m/z values. Beyond offering an orthogonal dimension of separation to RPLC, CZE can be directly interfaced with mass spectrometers via electrospray ionization (ESI), making it a useful tool for time- and cost-efficient online separations. Indeed, CZE has been employed to analyze antibody variants,[5] single protein proteoforms,[6] and even complex biological samples,[7,8] although advancements must still be made to address the inherent challenges of CZE-ESI integration. To improve CZE sensitivity, we recently developed an electrokinetically pumped sheath-flow nanospray CE-MS interface. This interface has been effective for various bottom-up proteomics experiments,[9−17] and we have also illustrated its value for top-down proteomics with both standard proteins mixtures[18] and complex protein samples derived from the *Mycobacterium marinum* bacterial secretome.[19]

Even as CZE technology rapidly improves for proteomic applications, this separation technique has yet to capitalize on the advantages of electron-driven dissociation, remaining one-dimensional in its exclusive use of canonical collision-based dissociation methods for protein characterization.[20−22] Electron-driven dissociation methods, e.g., electron capture dissociation (ECD)[23] and electron transfer dissociation (ETD),[24,25] have been a significant boon to intact protein analysis over the past 15 years, providing extensive cleavage of

Received: March 5, 2015
Accepted: April 20, 2015
Published: April 20, 2015

DOI: 10.1021/acs.analchem.5b00883
Anal. Chem. 2015, 87, 5422−5429

peptide and protein backbone bonds. These dissociation methods leverage electron rearrangements driven by capture of free, low-energy electrons (ECD) or transfer of an electron from radical reagent anions (ETD) to generate sequence-informative c- and z-type fragment ions. Both ECD and ETD retain labile PTMs and promote backbone bond cleavage largely independent of amino acid sequence, addressing several limitations intrinsic to the threshold-type dissociation mechanism of collision-based methods like collisionally activated dissociation (CAD)[26−29] and higher-energy collisional dissociation (HCD).[30,31] The transferability of ETD to any mass spectrometry platform with an rf trapping device has made it especially valuable as top-down proteomics continues to advance beyond a few specialized laboratories to more ubiquitous use in the proteomic community.[32−36]

The dependence of electron-driven dissociation efficiency on precursor charge density, however, has diminished the extent at which ETD can robustly fragment peptide and protein precursor cations with low charge density (i.e., higher m/z values).[37−39] As precursor m/z values increase, so increases the likelihood of nondissociative electron transfer (ETnoD),[40] a process in which backbone bond cleavage occurs but the fragment ions remain bound together by noncovalent interactions. ETnoD reduces precursor-to-product ion conversion, limiting the sequence information gleaned from an ETD MS/MS event. The secondary gas-phase structure responsible for ETnoD can be disrupted through addition of supplemental energy through resonant excitation, photoactivation, and elevated temperatures (collectively termed "activated ion" techniques), effectively increasing product ion yield. Inspired by successes of activated ion ECD (AI-ECD) methods[41−45] that mitigate nondissociative electron capture events using a variety of strategies, we and others have developed tools to increase peptide identifications with ETD using collisional activation of electron transfer products[46,47] as well as concurrent infrared photoactivation during ETD reactions.[48−50] The latter of these techniques, termed activated ion ETD (AI-ETD), has shown the greatest potential for increasing sequence-informative product ion generation because it not only minimizes problematic hydrogen abstraction but also incurs no additional time to the MS/MS scan event. Recently, we described the substantial benefits AI-ETD can offer for intact protein characterization,[51] but the boosts provided by AI-ETD have yet to be coupled with online separations for top- down proteomics.

In this work, we present the first study that demonstrates the compatibility of online CZE separations with ETD and AI-ETD methodologies. First, we compare the performance of HCD, conventional ETD, and AI-ETD for CZE-MS/MS experiments to analyze a mixture of four standard proteins, with molecular weights ranging from ∼12 to ∼29 kDa. ETD generated either comparable or greater numbers of matched fragments than HCD for three of the protein standards while maintaining higher spectra quality than HCD for all four proteins. AI-ETD extended the performance of ETD in several cases, generating more matching fragments and higher spectral quality than ETD and HCD. Following these studies, we analyzed complex protein mixtures from the secretome of *M. marinum*. Here we show that ETD and HCD can be performed in consecutive scans on the electrophoretic time scale, affording more than double the protein sequence coverage achieved with HCD fragmentation alone. Furthermore, AI-ETD outperformed the other fragmentation methods, identifying more proteins than ETD and generating higher quality tandem mass spectra than both ETD and HCD, sometimes accounting for even higher protein sequence coverage than ETD and HCD combined. In addition, the combination of fragments generated from AI-ETD and HCD scans improved sequence coverage by more than 3-fold over HCD alone. This work not only demonstrates the amenability of ion−ion reactions to the electrophoretic time scale, but also illustrates that ETD technology can greatly extend the analytical power CZE provides for the top-down approach.

EXPERIMENTAL SECTION

Materials and Reagents. All reagents were purchased from Sigma-Aldrich (St. Louis, MO, USA), unless stated otherwise. Formic acid (FA) and glacial acetic acid were purchased from Fisher Scientific (Pittsburgh, PA). Methanol was purchased from Honeywell Burdick & Jackson (Wicklow, Ireland). Water was deionized by a NanoPure system from Thermo Scientific (Marietta, OH). A linear polyacrylamide (LPA)-coated fused capillary (50 μm i.d. × 150 μm o.d.) was purchased from Polymicro Technologies (Phoenix, AZ).

Sample Preparation. A standard protein mixture was prepared by dissolving cytochrome c, myoglobin, carbonic anhydrase and β-casein in 0.08% FA, 20% acetonitrile in water with concentrations of 0.06, 0.06, 0.12, and 0.4 mg/mL, respectively. The culturing of *M. marinum* and generation of short- term culture filtrates have been described elsewhere.[52] A secreted protein fraction containing approximately 100 μg of protein, as determined by the bicinchoninic acid assay, was purified by ice-cold acetone precipitation and resuspended in 30 μL 30% acetic acid, 30% acetonitrile in water.

CZE-ESI-MS/MS Analysis. CZE was coupled to an ETD-enabled Orbitrap Elite mass spectrometer (Thermo Fisher Scientific, San Jose, CA) that included a multipurpose dissociation cell (MDC), permitting HCD, ETD, and AI-ETD to occur all in the same reaction vessel.[51] Electrospray was generated using an electrokinetically pumped sheath flow through a nanospray emitter.[14] The borosilicate glass emitter (1.0 mm o.d. × 0.75 mm i.d., 10 cm length) was pulled with a Sutter instrument P-1000 flaming/brown micropipet puller. The emitter inner diameter was 10−12 μm. Separation was performed in a 50 cm long, 50 μm ID, 150 μm OD LPA-coated fused capillary. The separation buffer was 0.1% (v/v) FA. The electrospray sheath liquid was 10% (v/v) methanol and 0.1% (v/v) FA. About 35 nL of standard protein solution or 70 nL of secretome solution was injected for each experiment. The separation voltages were 26 and 14 kV for standard proteins and secretome, respectively. The inlet ion transfer tube was held at 275 °C and the S-lens rf level was set at 60%. Full MS scans were acquired in the Orbitrap over the m/z 500−1500 range with a resolving power of 60,000 at m/z 400. The three most intense peaks with charge state ≥4 were selected in data-dependent fashion for fragmentation. A normalized collision energy of 25 was used for HCD, whereas ETD and AI-ETD reaction times were set to 10 ms and fluoranthene reagent anions were accumulated for 15 ms prior to the ion−ion reactions. During AI-ETD reactions, an external Firestar T-100 Synrad 100-W CO_2 continuous wave laser (Mukilteo, WA) was triggered using instrument firmware and modification to instrument code in conjunction with a gated laser controller. The laser irradiated the trapping volume of the MDC during the entirety of the ETD reaction and 70% total output. For all AI-ETD experiments, the nitrogen pressure in the MDC was lowered to a ΔN_2 pressure of $\sim 0.1 \times 10^{-10}$ Torr, as measured by the Penning gauge in the Orbitrap chamber, to prevent collisional cooling that negates the additional energy supplied by the infrared laser. Gas pressure was left at normal operating levels for HCD and ETD scans to ensure proper collisional dissociation (ΔN_2 of $\sim 0.3 \times 10-10$ Torr). Detection for all tandem mass spectra was performed in the Orbitrap with a resolving power of 30 000 at m/z 400. The MS^1 AGC target value was 1 000 000 with a maximum injection time of 100 ms, whereas MS/MS scans have an AGC target value of 500 000 and a maximum injection time of 500 ms. Three microscans were used in both MS and MS/MS scans. An

DOI: 10.1021/acs.analchem.5b00883
Anal. Chem. 2015, 87, 5422−5429

exclusion window of ±10 ppm was constructed around the monoisotopic peak of each selected precursor for 30 s.

Data Analysis. Raw files analyzing the standard protein mixture were first converted to mzXML files with ReAdW (version 4.3.1), whereas raw files from secretome analysis were separated based on a fragmentation method (HCD/ETD) and converted to mzXML files with msConvert. Tandem spectra were then decharged and deisotoped by MS-Deconv (version 0.8.0.7370),[53] followed by database searching with MS-Align+ software (version 0.7.1.7143),[54] using *b*- and *y*-type ions for HCD searches and *c*- and *z*-type ions for ETD and AI-ETD. A custom database including four model proteins (bovine cytochrome c, equine myoglobin, bovine carbonic anhydrase, and bovine *β*-casein) was used for standard protein mixture analysis. An NCBI protein database for *M. marinum* secretome including common contaminates (5583 protein sequences) was used for secretome analysis. The parameters for both database searches included maximum number of modifications (shift number) as 2, mass error tolerance as 10 ppm, "doOneDaltonCorrection" and "doChargeCorrection" as false, "cutoffType" as EVALUE, and cutoff as 0.001. *E*-value estimates the probability of observing a similar matching by chance in a database of the current size.

RESULTS AND DISCUSSION

Benchmarking the Compatibility of Ion−Ion Reactions with CZE-MS/MS. Prior to this study, CZE separations have exclusively employed collision-based fragmentation methods for MS/MS analysis. Given the value of CZE and electron-driven dissociation for intact protein separations and fragmentation, respectively, we recognized the potential such a combination could have for top-down proteomics, presenting herein the first study to couple the two technologies. We first evaluated the performance of ETD on the electrophoretic time scale by analyzing a standard protein mixture, using a CZE-MS/MS analysis of the same mixture but with HCD fragmentation as a reference point for comparison. This protein mixture contained cytochrome c, myoglobin, carbonic anhydrase, and *β*-casein, representing the molecular weight range of proteins seen in typical top-down experiments (<30 kDa). Similar to our previous results with CZE separations of a standard protein mixture, all four proteins were nearly baseline resolved, and three peaks were resolved for *β*-casein, which indicates that at least three proteoforms were separated (Figure 1, panel A). ETD MS/MS events typically require slightly longer scan times than HCD analyses to allow for sufficient ETD reaction time. Longer scan times result in fewer tandem mass spectra collected over the migration profile of a given protein, which can challenge the robustness of a top-down experiment. Panel B of Figure 1 shows the number of MS/MS scans that were collected over the migration profile of each of the protein standards. As expected, ETD tandem mass spectra averaged marginally longer scan times than those performed with HCD (1.38 s/scan vs 1.21 s/scan), and fewer MS/MS scans were acquired for most of the proteins. Despite this small drop in scan acquisition, all four proteins were identified with both ETD and HCD.

Knowing that scan speed requirements of ETD provide successful top-down analysis with CZE separations, we also analyzed the standard protein mixture using AI-ETD fragmentation, which also identified all proteins in the mixture. Table 1 summarizes the results achieved with all three fragmentation methods (HCD, ETD, and AI-ETD). The detailed proteoform masses are listed in Table S1 of the Supporting Information. ETD substantially outperformed HCD in product ion generation for the relatively smaller proteins cytochrome c and myoglobin (both <17 kDa), while

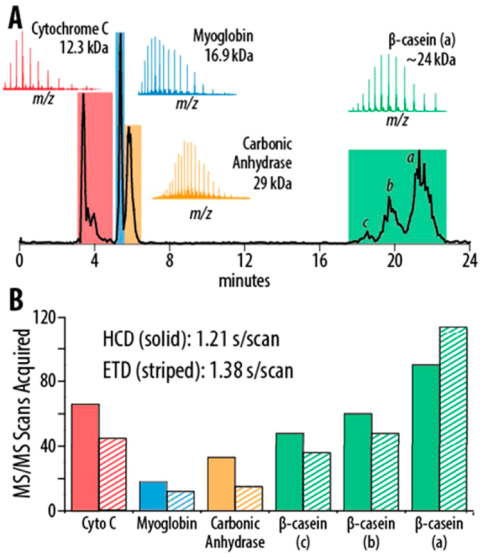

Figure 1. Capillary zone electrophoresis on an ETD-enabled Orbitrap system. (A) Base peak electropherogram of four standard proteins separated by the CZE-ESI-MS/MS system, including three proteoforms of *β*-casein (labeled a−c). Colored MS^1 spectra correspond to migration profiles of the designated proteins. (B) Comparison of number of tandem mass spectra acquired for each protein standard using either HCD or ETD, with average time per MS/MS scan provided.

maintaining comparable production of matching fragments for *β*-casein (~24 kDa) and carbonic anhydrase (~29 kDa). Furthermore, ETD out performed HCD in spectral quality for these standard proteins, producing higher matching percentages (number of matched fragments divided by total number of ions in the spectrum) for all four proteins. This difference is likely explained by the high energy deposition in the HCD process, which often generates ammonia and water neutral losses in addition to a-type ions and low mass internal fragments produced by multiple backbone cleavages (all of which are not included in the MS-Align+ database search). AI-ETD expanded the benefits of ETD even further, generating more matching fragments than ETD for cytochrome C and carbonic anhydrase, and also surpassing the matching percentages (i.e., spectral quality) of both ETD and HCD for three of the four proteins. Fragmentation of *β*-casein with AI-ETD, however, produced suboptimal results, even though HCD and ETD performed similarly to each other. This may be due to several idiosyncratic characteristics of *β*-casein, including high levels of phosphorylation (up to five modifications within a 21 residue stretch) and a strikingly proline-rich sequence, both of which can cause unpredicted fragmentation in the presence of IR irradiation. Regardless, these electron-driven dissociation methods provided commensurate, if not superior fragmentation of these four standard proteins compared to HCD. Additionally, AI-ETD often enhanced the results ETD could provide, granted further experiments outside the scope of this study are required to determine the amenability of AI-ETD to proteins with uncommon traits, such as *β*-casein.

Complementary Fragmentation Methods for Top-Down CZE-MS/MS. Practitioners of top-down proteomics often leverage the complementary fragmentation achieved with ETD and HCD to improve protein characterization. When comparing sites of backbone cleavage in the standard protein sequences, relatively few fragmentation sites overlap between

DOI: 10.1021/acs.analchem.5b00883
Anal. Chem. 2015, 87, 5422−5429

Table 1. Number of Identified Isoforms and Matched/Unmatched Fragment Ions of the Best PrSMs of the Four Standard Proteins

	cytochrome c			myoglobin			carbonic anhydrase			β-casein		
	HCD	ETD	AI-ETD	HCD	ETD	AI-ETD	HCD	ETD	AI-ETD	HCD	ETD	AI-ETD
matched/total fragment ions	50/147	85/203	102/203	21/214	67/157	54/115	63/215	52/145	58/125	39/147	38/81	20/107
percentage of matching	34%	42%	50%	9.8%	43%	47%	29%	36%	46%	27%	47%	19%
number of proteoforms	9	5	5	2	2	2	21	8	8	18	24	11

ETD and HCD, reflecting the inherent differences in their dissociation mechanisms. The majority of cleavage sites seen with ETD and AI-ETD are the same, unsurprising, as AI-ETD is merely an enhancement of the ETD reaction. Figure 2

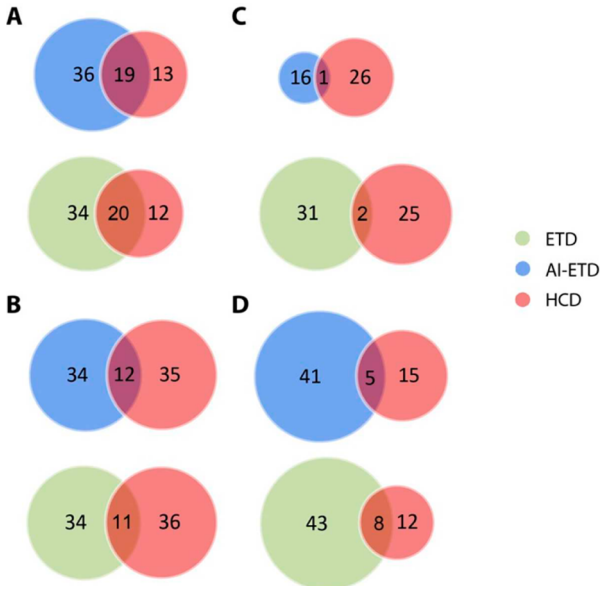

Figure 2. Overlap of fragmentation sites from AI-ETD and HCD spectra for cytochrome c (A), carbonic anhydrase (B), β-casein (C), and myoglobin (D).

highlights the amount overlap (or lack thereof) in fragmentation sites between the three methods, and Figure S1 of the Supporting Information shows sequence maps depicting bond cleavages for the best protein spectral matches (PrSMs) with their tandem MS spectra for each standard protein. Combining the total backbone cleavages achieved separately with HCD and ETD afforded sequence coverage gains of 106% for cytochrome c, 215% for myoglobin, 115% for β-casein, and 72% for carbonic anhydrase over HCD alone (Figure S2 of the Supporting Information), demonstrating the improvements in protein characterization ETD can provide for current CZE-MS/MS approaches. The protein sequence coverage in this paper is backbone bond coverage, defined as a percentage that represents the number backbone bonds cleaved divided by total number of backbone bonds.

AI-ETD further bolstered these gains in protein sequence coverage, as shown in Figure 3. Cytochrome c achieved near complete coverage across the entire sequence, excluding the region surrounding the heme group binding domain. The combination of AI-ETD/HCD fragments increased sequence coverage of carbonic anhydrase and β-casein by 72% and 60%, respectively. The most remarkable improvement in sequence coverage was achieved with myoglobin, as the combination of AI-ETD and HCD increased sequence coverage greater than 3-fold over fragmentation solely with HCD (from 13% to 40%). HCD has been shown to provide less extensive fragmentation of myoglobin due to preferential cleavages that arise from the protein's globular nature with regions of varying disorder,[55] which suggests that the addition of alternative fragmentation methods like ETD and AI-ETD is crucial for sufficient characterization. Altogether, these improvements in sequence coverage highlight the compatibility of CZE protein separations to novel fragmentation methods like AI-ETD and also demonstrate the extensive protein characterization that can

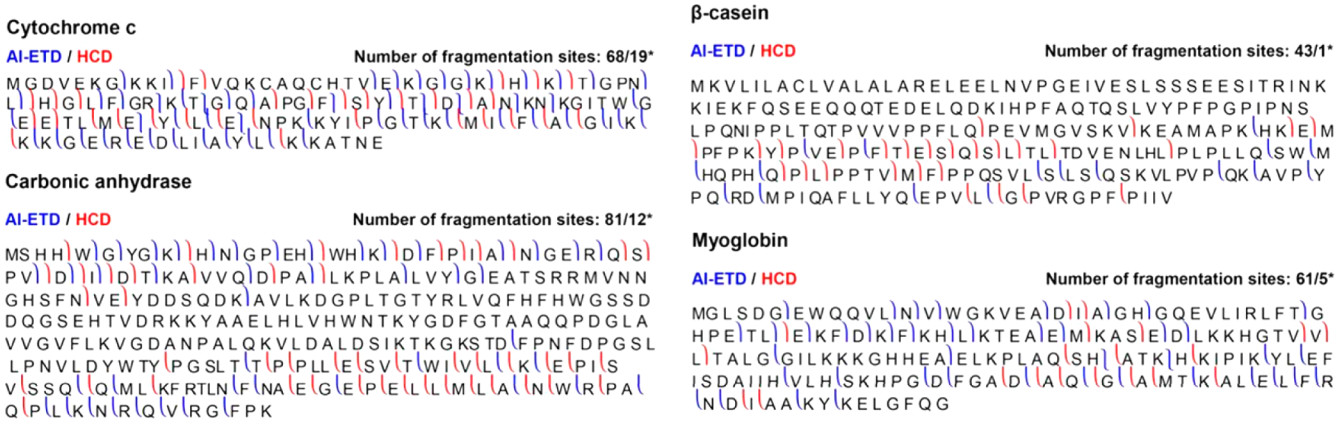

Figure 3. Sequence maps show combined fragmentation patterns of AI-ETD and HCD for cytochrome c (top left), carbonic anhydrase (bottom left), β-casein (top right)m and myoglobin (bottom right). *Number of fragmentation sites: total fragmentation sites/overlapped fragmentation sites.

DOI: 10.1021/acs.analchem.5b00883
Anal. Chem. 2015, 87, 5422−5429

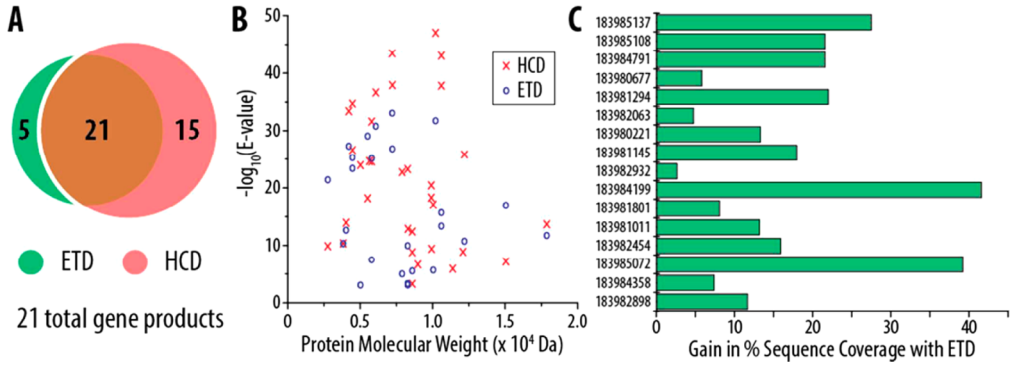

Figure 4. Analysis of *M. marinum* secretome with ETD and HCD, Run 1. (A) The overlap in proteoforms identified using back-to-back ETD/HCD scans in a single CZE-MS/MS run, mapping to a total of 21 gene products. (B) Identification score (E-value) versus protein molecular weight for proteoforms identified with ETD and HCD. (C) Gain in percent sequence coverage when using a combination of fragments from an ETD scan and an HCD scan together over the sequence coverage achieved with HCD alone. Proteins on the *y*-axis are identified by their accession number.

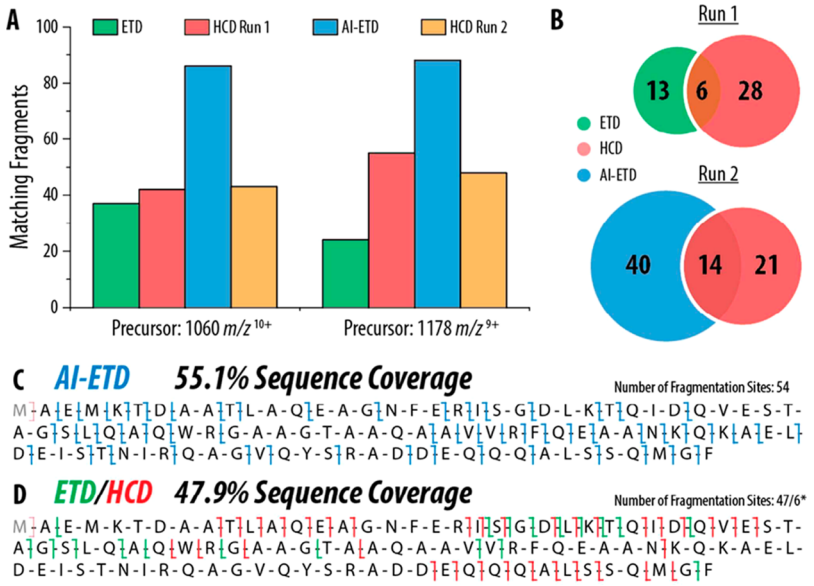

Figure 5. Comparison of fragmentation quality using HCD, ETD, and AI-ETD for the characterization of 10 kDa culture filtrate antigen EsxB_1, a protein known to play a role in virulence in *M. marium*. (A) The number of matching fragments generated by the three fragmentation methods at two different precursors of antigen EsxB_1. HCD results from both Run 1 (which included ETD scans) and Run 2 (which included AI-ETD scans) are included. (B) Overlap of fragmentation sites using ETD and HCD spectra from Run 1, and using AI-ETD and HCD spectra from Run 2. (C) Sequence map depicting the bonds cleaved by AI-ETD alone in a single MS/MS scan. (D) Sequence map depicting the bonds cleaved by a combination fragments from an ETD scan and HCD scan. *Total bonds cleaved/shared cleavage sites.

be achieved using electron-driven dissociation techniques with online CZE separations.

Evaluating the Combination of ETD and HCD for Top-Down Proteomics on the *M. marinum* Secretome. We followed these standard protein studies with by expanding our experimental scope to a more complex, biologically relevant protein mixture derived from the *Mycobacterium marinum* secretome. This opportunistic pathogen is regularly used as a model system for studying more insidious pathogens like *Mycobacterium tuberculosis*, which is the causative agent of most cases of tuberculosis.[52,56−58] Virulence of these bacterial species is thought to be a function of secreted proteins, although the exact causes are unknown and remain an area of active research. Additionally, the pool of proteins contained in the *M. marinum* secretome span a relatively small range of protein molecular weights (<30 kDa), providing an ideal system to use as a test bed for our ETD-enabled CZE-MS/MS platform.[19] Capitalizing on the success we saw above using ETD and HCD as complementary fragmentation techniques, we performed a 60 min CZE separation using the two dissociation methods in tandem. Precursors were selected in data-dependent fashion from a high-resolution MS^1 scan performed in the Orbitrap, followed by three pairs of sequential HCD and ETD tandem mass spectra, for a total of six MS/MS events per cycle. Figure 4 summarizes the results of this analysis, whereas Figure S3 (top) and Table S2 of the Supporting Information provide the base peak electropherogram and identified protein groups, respectively. The proteoforms lists in Tables S2 and S3 of the Supporting Information reflect the database searching results from Ms-Align+ software. However, those proteoforms with ∼1 Da mass difference could be the same protein species, which can results from errors during deconvolution. The total number of proteoforms would be ∼85% of the listed one if those Δ1 Da proteoforms are excluded. Because ETD and HCD generate different product ion types, tandem mass spectra from the two respective dissociation methods were searched separately

DOI: 10.1021/acs.analchem.5b00883
Anal. Chem. 2015, 87, 5422−5429

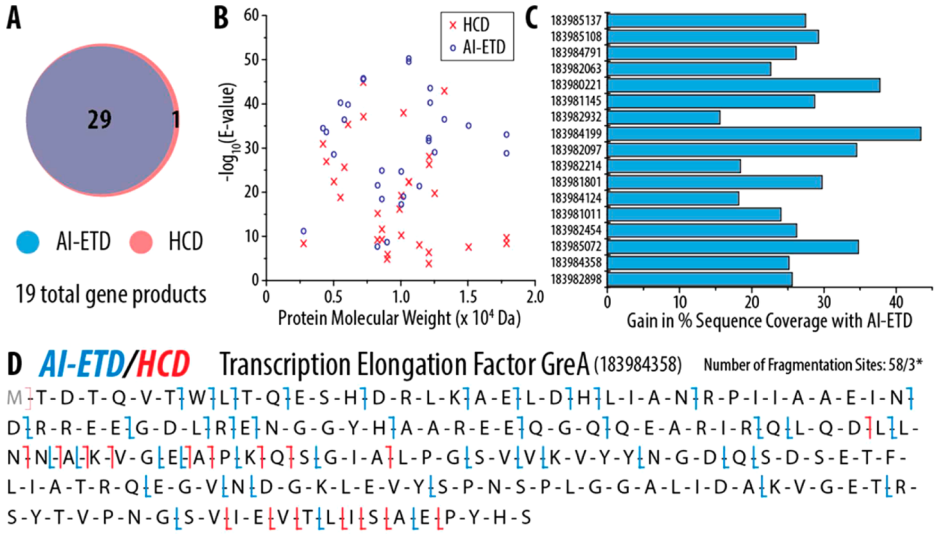

Figure 6. Analysis of *M. marinum* secretome with AI-ETD and HCD, Run 2. (A) The overlap in proteoforms identified using back-to-back AI-ETD/HCD scans in a single CZE-MS/MS run, mapping to a total of 19 gene products. (B) Identification score (E-value) versus protein molecular weight for proteoforms identified with AI-ETD and HCD. (C) Gain in percent sequence coverage when using a combination of fragments from an AI-ETD scan and an HCD scan together over the sequence coverage achieved with HCD alone. Proteins on the *y*-axis are identified by their accession number. (D) Sequence map depicting the number of bonds cleaved for Transcription Elongation Factor GreA (accession number: 183984358), explained by a combination of fragments generated from an AI-ETD scan and an HCD scan. *Total bonds cleaved/shared cleavage sites.

against a complete *M. marinum* database using MS-Align+. ETD identified 26 total proteoforms, while HCD performed better, characterizing 36 proteoforms. Altogether, ETD and HCD accounted for 41 proteoforms, corresponding to 21 unique gene products (panel A, Figure 4). This analysis produced fewer proteoform identifications but nearly the same number of total gene product identifications as our previous CZE-MS/MS analyses using solely HCD. This reduction in number of identified proteoforms is attributed to the redundant precursor sampling of subsequent HCD and ETD scans, although this sampling did not adversely affect the number gene products characterized.

HCD spectra generally earned better identification scores, i.e., *E*-values, than ETD spectra (panel B, Figure 4), although the quality of ETD spectra could be improved in future studies through more judicious selection of ETD reaction parameters, such as reaction duration and reagent anion accumulation time. Regardless, the addition of ETD to the CZE-MS/MS platform still provided considerable advantages. Panel C of Figure 4 displays the gain in percent protein sequence coverage that was contributed by the addition of ETD fragmentation over HCD alone for 16 gene products detected with both methods. This value does not represent a fold-change measurement but rather depicts the raw difference in percent sequence coverage observed. For example, iron-regulated Lsr2 protein (a protein involved in the iron-dependent protein secretion implicated in bacterial virulence,[59,60] accession number 183982454) had a sequence coverage of only 15.2% with HCD fragmentation. When fragments generated from HCD were combined with fragments from ETD, this sequence coverage improved to 31.1%, a gain in raw present sequence coverage of ∼16% (corresponding to a more than 2-fold improvement). These results illustrate that ETD can be coupled with HCD in sequential scans on the electrophoretic time scale, improving protein characterization achievable with front-end CZE separations.

Advantages of AI-ETD for Top-Down CZE-MS/MS on Complex Proteins Mixtures. Spring-boarding from the success of combining subsequent ETD and HCD in a single CZE-MS/MS experiment, we then analyzed the *M. marium* secretome protein mixture with a combination of AI-ETD and HCD in the same fashion. The CZE separations were highly reproducible (Figure S3 of the Supporting Information), and many proteins that were detected in the first ETD/HCD analysis (Run 1) were also identified in the AI-ETD/HCD experiment (Run 2), enabling the comparison of ETD, AI-ETD, and HCD for shotgun top-down proteomics. Figure 5 encapsulates these comparisons, showing results for *M. marinum* protein 10 kDa culture filtrate EsxB_1 (accession number 183980221). This protein is directly connected with *M. marinum* virulence through involvement in a novel secretion apparatus and is in a family of proteins targeted in current tuberculosis research.[52,59] Panel A of Figure 5 shows that AI-ETD maintained optimal product ion generation over both ETD and HCD, even as precursor charge density decreased. For the +10 precursor, ETD and AI-ETD both provided complementary fragmentation to HCD (Panel B, Figure 5), although AI-ETD substantially increased the number of total fragmentation sites over ETD and HCD alone (54 with AI-ETD vs 19 with ETD, 34 with HCD Run 1, and 35 with HCD Run 2). As described above, the combination of ETD and HCD fragments improved sequence coverage over HCD alone (from ∼35% to ∼48%), but AI-ETD still afforded the highest sequence coverage on its own (∼55%), even over the combination of ETD and HCD (Panels C and D, Figure 5).

For a more holistic evaluation of the combination of AI-ETD and HCD in the same experiment, Figure 6 summarizes the results of Run 2 and permits straightforward comparisons to ETD/HCD performance in Run 1. Protein identifications from Run 2 are provided in Table S3 of the Supporting Information. AI-ETD identified more proteoforms (29) than ETD, although the overlap in identifications between AI-ETD and HCD in Run 2 was higher than ETD/HCD overlap seen in Run 1

DOI: 10.1021/acs.analchem.5b00883
Anal. Chem. 2015, 87, 5422−5429

(Panel A, Figure 6). As with the standard protein analysis above, AI-ETD outperformed HCD in spectral quality in Run 2, generally affording better identification scores for proteins across the molecular weight range observed (Panel B, Figure 6). AI-ETD also significantly improved the quality of tandem mass spectra acquired over ETD in Run 1, with average *E*-values of 7.3×10^{-10} and 1.0×10^{-4}), respectively, while HCD identifications score remained relatively constant between the two experiments (Run 1 average of 1.4×10^{-5} and Run 2 average of 4.8×10^{-6}). Combining fragments from AI-ETD and HCD typically increased gains in percent protein sequence coverage (Panel C, Figure 6) more than the ETD/HCD combinations from Run 1. Panel D of Figure 6 shows the extensive sequence coverage achieved from the AI-ETD/HCD combination for transcription elongation factor GreA (accession number 183984358). Here HCD provided to 19 total fragmentation sites, or 11.65% sequence coverage. The addition of AI-ETD fragments contributed a gain in sequence coverage of over 25%, a more than 3-fold improvement in sequence coverage. These results show that AI-ETD is a robust fragmentation method for improved ETD performance that can be used in top-down experiments on its own or can be complemented by HCD for even further enhancement in protein characterization.

CONCLUSIONS

In this study, we have described the first implementation of front-end CZE separations with ETD, leveraging the strengths of both for top-down protein analysis of simple and complex protein mixtures. Furthermore, we have shown that CZE separations are also compatible with novel dissociation techniques like AI-ETD for enhanced intact protein fragmentation, showing the impact AI-ETD can have in improving top-down results. Importantly, we also demonstrate that electron-driven dissociation methods like ETD and AI-ETD can be coupled in tandem with collision-based fragmentation (e.g., HCD) in the same CZE-MS/MS analysis, offering superior protein characterization via complementary fragmentation mechanisms on the electrophoretic time scale. Ultimately, this work highlights the compelling potential electron-driven dissociation methods have for top-down proteomics with CZE separations, opening new possibilities for intact protein analysis.

ASSOCIATED CONTENT

Supporting Information

Additional information as noted in text. The Supporting Information is available free of charge on the ACS Publications website at DOI: 10.1021/acs.analchem.5b00883.

AUTHOR INFORMATION

Corresponding Author

*N. J. Dovichi. Tel.: +1 574-631-2778. E-mail: ndovichi@nd.edu.

Author Contributions

⊥Y.Z. and N.M.R. contributed equally to this manuscript and are cofirst authors.

Notes

The authors declare no competing financial interest.

ACKNOWLEDGMENTS

This work was funded by the National Institutes of Health (R01GM096767-NJD) and (R01GM080148-JJC). N.M.R. gratefully acknowledges support of an NSF graduate fellowship (DGE-1256259).

REFERENCES

(1) Valaskovic, G. A.; Kelleher, N. L.; McLafferty, F. W. *Science* **1996**, *273*, 1199−1201.
(2) Simo, C.; Herrero, M.; Neususs, C.; Pelzing, M.; Kenndler, E.; Barbas, C.; Ibanez, E.; Cifuentes, A. *Electrophoresis* **2005**, *26*, 2674−2683.
(3) Jorgenson, J. W.; Lukacs, K. D. *Science* **1983**, *222*, 266−272.
(4) Han, X. M.; Jin, M.; Breuker, K.; McLafferty, F. W. *Science* **2006**, *314*, 109−102.
(5) Haselberg, R.; de Jong, G. J.; Somsen, G. W. *Anal. Chem.* **2013**, *85*, 2289−2296.
(6) Yang, Y.; Barendregt, A.; Kamerling, J. P.; Heck, A. J. *Anal. Chem.* **2013**, *85*, 12037−12045.
(7) Li, Y.; Compton, P. D.; Tran, J. C.; Ntai, I.; Kelleher, N. L. *Proteomics* **2014**, *14*, 1158−1164.
(8) Han, X.; Wang, Y.; Aslanian, A.; Bern, M.; Lavallee-Adam, M.; Yates, J. R., 3rd. *Anal. Chem.* **2014**, *86*, 11006−12.
(9) Li, Y.; Champion, M. M.; Sun, L.; Champion, P. A.; Wojcik, R.; Dovichi, N. J. *Anal. Chem.* **2012**, *84*, 1617−1622.
(10) Li, Y.; Wojcik, R.; Dovichi, N. J.; Champion, M. M. *Anal. Chem.* **2012**, *84*, 6116−6121.
(11) Mou, S.; Sun, L.; Dovichi, N. J. *Anal. Chem.* **2013**, *85*, 10692−10696.
(12) Mou, S.; Sun, L.; Wojcik, R.; Dovichi, N. J. *Talanta* **2013**, *116*, 985−990.
(13) Sun, L.; Zhu, G.; Li, Y.; Wojcik, R.; Yang, P.; Dovichi, N. J. *Proteomics* **2012**, *12*, 3013−3019.
(14) Sun, L.; Zhu, G.; Zhao, Y.; Yan, X.; Mou, S.; Dovichi, N. J. *Angew. Chem., Int. Ed. Engl.* **2013**, *52*, 13661−13664.
(15) Wojcik, R.; Dada, O. O.; Sadilek, M.; Dovichi, N. J. *Rapid Commun. Mass Spectrom.* **2010**, *24*, 2554−2560.
(16) Yan, X.; Essaka, D. C.; Sun, L.; Zhu, G.; Dovichi, N. J. *Proteomics* **2013**, *13*, 2546−2551.
(17) Sun, L.; Hebert, A. S.; Yan, X.; Zhao, Y.; Westphall, M. S.; Rush, M. J.; Zhu, G.; Champion, M. M.; Coon, J. J.; Dovichi, N. J. *Angew. Chem., Int. Ed.* **2014**, *53*, 13931−13933.
(18) Sun, L.; Knierman, M. D.; Zhu, G.; Dovichi, N. J. *Anal. Chem.* **2013**, *85*, 5989−5995.
(19) Zhao, Y.; Sun, L.; Champion, M. M.; Knierman, M. D.; Dovichi, N. J. *Anal. Chem.* **2014**, *86*, 4873−4878.
(20) Jensen, P. K.; Pasa-Tolic, L.; Anderson, G. A.; Horner, J. A.; Lipton, M. S.; Bruce, J. E.; Smith, R. D. *Anal. Chem.* **1999**, *71*, 2076−2084.
(21) Sun, L. L.; Zhu, G. J.; Yan, X. J.; Champion, M. M.; Dovichi, N. J. *Proteomics* **2014**, *14*, 622−628.
(22) Mischak, H.; Coon, J. J.; Novak, J.; Weissinger, E. M.; Schanstra, J. P.; Dominiczak, A. F. *Mass Spectrom. Rev.* **2009**, *28*, 703−724.
(23) Zubarev, R. A.; Kelleher, N. L.; McLafferty, F. W. *J. Am. Chem. Soc.* **1998**, *120*, 3265−3266.
(24) Syka, J. E. P.; Coon, J. J.; Schroeder, M. J.; Shabanowitz, J.; Hunt, D. F. *Proc. Nat. Acad. Sci. U. S. A.* **2004**, *101*, 9528−9533.
(25) Coon, J. J.; Ueberheide, B.; Syka, J. E. P.; Dryhurst, D. D.; Ausio, J.; Shabanowitz, J.; Hunt, D. F. *Proc. Nat. Acad. Sci. U. S. A.* **2005**, *102*, 9463−9468.
(26) Hunt, D. F.; Buko, A. M.; Ballard, J. M.; Shabanowitz, J.; Giordani, A. B. *Biomed. Mass Spectrom.* **1981**, *8*, 397−408.
(27) McLuckey, S. A. *J. Am. Soc. Mass Spectrom.* **1992**, *3*, 599−614.
(28) Verentchikov, A. N.; Ens, W.; Standing, K. G. *Anal. Chem.* **1994**, *66*, 126−133.
(29) Morris, H. R.; Paxton, T.; Dell, A.; Langhorne, J.; Berg, M.; Bordoli, R. S.; Hoyes, J.; Bateman, R. H. *Rapid Commun. Mass Spectrom.* **1996**, *10*, 889−896.
(30) Wysocki, V. H.; Tsaprailis, G.; Smith, L. L.; Breci, L. A. *J. Mass Spectrom.* **2000**, *35*, 1399−1406.
(31) Olsen, J. V.; Macek, B.; Lange, O.; Makarov, A.; Horning, S.; Mann, M. *Nat. Methods* **2007**, *4*, 709−712.

DOI: 10.1021/acs.analchem.5b00883
Anal. Chem. 2015, 87, 5422−5429

(32) Mikesh, L. M.; Ueberheide, B.; Chi, A.; Coon, J. J.; Syka, J. E. P.; Shabanowitz, J.; Hunt, D. F. *Biochim. Biophys. Acta* **2006**, *1764*, 1811−1822.
(33) McAlister, G. C.; Phanstiel, D.; Good, D. M.; Berggren, W. T.; Coon, J. J. *Anal. Chem.* **2007**, *79*, 3525−3534.
(34) Catherman, A. D.; Skinner, O. S.; Kelleher, N. L. *Biochem. Biophys. Res. Commun.* **2014**, *445*, 683−693.
(35) Gregorich, Z. R.; Ge, Y. *Proteomics* **2014**, *14*, 1195−1210.
(36) Smith, L. M.; Kelleher, N. L. *Nat. Methods* **2013**, *10*, 186−187.
(37) Good, D. M.; Wirtala, M.; McAlister, G. C.; Coon, J. J. *Mol. Cell. Proteomics* **2007**, *6*, 1942−1951.
(38) Valentine, S. J.; Counterman, A. E.; Clemmer, D. E. *J. Am. Soc. Mass Spectrom.* **1997**, *8*, 954−961.
(39) Breuker, K.; Oh, H.; Horn, D. M.; Cerda, B. A.; McLafferty, F. W. *J. Am. Chem. Soc.* **2002**, *124*, 6407−6420.
(40) Han, H. L.; Xia, Y.; McLuckey, S. A. *Rapid Commun. Mass Spectrom.* **2007**, *21*, 1567−1573.
(41) Oh, H.; Breuker, K.; Sze, S. K.; Ge, Y.; Carpenter, B. K.; McLafferty, F. W. *Proc. Natl. Acad. Sci. U. S. A.* **2002**, *99*, 15863−15868.
(42) Oh, H. B.; McLafferty, F. W. *Bull. Korean Chem. Soc.* **2006**, *27*, 389−394.
(43) Ben Hamidane, H.; Chiappe, D.; Hartmer, R.; Vorobyev, A.; Moniatte, M.; Tsybin, Y. O. *J. Am. Soc. Mass Spectrom.* **2009**, *20*, 567−575.
(44) Mikhailov, V. A.; Cooper, H. J. *J. Am. Soc. Mass Spectrom.* **2009**, *20*, 763−771.
(45) Horn, D. M.; Ge, Y.; McLafferty, F. W. *Anal. Chem.* **2000**, *72*, 4778−4784.
(46) Swaney, D. L.; McAlister, G. C.; Wirtala, M.; Schwartz, J. C.; Syka, J. E. P.; Coon, J. J. *Anal. Chem.* **2007**, *79*, 477−485.
(47) Xia, Y.; Han, H.; McLuckey, S. A. *Anal. Chem.* **2008**, *80*, 1111−1117.
(48) Ledvina, A. R.; Rose, C. M.; McAlister, G. C.; Syka, J. E. P.; Westphall, M. S.; Griep-Raming, J.; Schwartz, J. C.; Coon, J. J. *J. Am. Soc. Mass Spectrom.* **2013**, *24*, 1623−1633.
(49) Ledvina, A. R.; McAlister, G. C.; Gardner, M. W.; Smith, S. I.; Madsen, J. A.; Schwartz, J. C.; Stafford, G. C., Jr.; Syka, J. E.; Brodbelt, J. S.; Coon, J. J. *Angew. Chem., Int. Ed.* **2009**, *48*, 8526−8528.
(50) Ledvina, A. R.; Beauchene, N. A.; McAlister, G. C.; Syka, J. E. P.; Schwartz, J. C.; Griep-Raming, J.; Westphall, M. S.; Coon, J. J. *Anal. Chem.* **2010**, *82*, 10068−10074.
(51) Riley, N. M., Westphall, M. S., Coon, J. J. Activated Ion Electron Transfer Dissociation for Improved Fragmentation of Intact Proteins. 2015, unpublished results.
(52) Champion, P. A.; Champion, M. M.; Manzanillo, P.; Cox, J. S. *Mol. Microbiol.* **2009**, *73*, 950−962.
(53) Liu, X. W.; Inbar, Y.; Dorrestein, P. C.; Wynne, C.; Edwards, N.; Souda, P.; Whitelegge, J. P.; Bafna, V.; Pevzner, P. A. *Mol. Cell. Proteomics* **2010**, *9*, 2772−2782.
(54) Liu, X. W.; Sirotkin, Y.; Shen, Y. F.; Anderson, G.; Tsai, Y. S.; Ting, Y. S.; Goodlett, D. R.; Smith, R. D.; Bafna, V.; Pevzner, P. A. *Mol. Cell. Proteomics* **2012**, *11*, No. M111.008524.
(55) Cammarata, M. B.; Brodbelt, J. S. *Chem. Sci.* **2015**, *6*, 1324−1333.
(56) Champion, P. A. D.; Stanley, S. A.; Champion, M. M.; Brown, E. J.; Cox, J. S. *Science* **2006**, *313*, 1632−1636.
(57) Cole, S. T.; Brosch, R.; Parkhill, J.; Garnier, T.; Churcher, C.; Harris, D.; Gordon, S. V.; Eiglmeier, K.; Gas, S.; Barry, C. E.; Tekaia, F.; Badcock, K.; Basham, D.; Brown, D.; Chillingworth, T.; Connor, R.; Davies, R.; Devlin, K.; Feltwell, T.; Gentles, S.; Hamlin, N.; Holroyd, S.; Hornby, T.; Jagels, K.; Krogh, A.; McLean, J.; Moule, S.; Murphy, L.; Oliver, K.; Osborne, J.; Quail, M. A.; Rajandream, M. A.; Rogers, J.; Rutter, S.; Seeger, K.; Skelton, J.; Squares, R.; Squares, S.; Sulston, J. E.; Taylor, K.; Whitehead, S.; Barrell, B. G. *Nature* **1998**, *393*, 537−544.
(58) Kennedy, G. M.; Hooley, G. C.; Champion, M. M.; Medie, F. M.; Champion, P. A. D. *J. Bacteriol.* **2014**, *196*, 1877−1888.
(59) Ratledge, C. *Tuberculosis* **2004**, *84*, 110−130.
(60) Bartek, I. L.; Woolhiser, L. K.; Baughn, A. D.; Basaraba, R. J.; Jacobs, W. R.; Lenaerts, A. J.; Voskuil, M. I. *mBio* **2014**, *5*, No. e01106-14.

DOI: 10.1021/acs.analchem.5b00883
Anal. Chem. 2015, 87, 5422−5429